CIMAC CONGRESS 25
ZURICH, MAY 19 – 23, 2025

2025 | 502

Preliminary implementation of a FC-ICE system for power and propulsion of a 14,000 TEU container ship

System Integration & Hybridization

Peter de Vos, Delft University of Technology

Niels de Vries, C-Job Naval Architects
Mees Feijen, Delft University of Technology
Joep van den Berg, Delft University of Technology
Britt van Lierop, Delft University of Technology
Jesse Zwart, Delft University of Technology

DOI: https://doi.org/10.5281/zenodo.15222942

ABSTRACT

This paper presents fast time-domain propulsion system simulation models for the Duisberg Test Case (DTC) post-Panamax container vessel using both diesel and ammonia as a fuel. The paper also provides first results of a ship integration study, demonstrating how the innovative combined SOFC-ICE AmmoniaDrive power plant could be integrated into the ship design.

With the first propulsion system model presented, voyages of the DTC container vessel are simulated while operating on regular marine diesel fuel, i.e., VLSFO, in a regular marine two-stroke diesel engine. In other words, this model provides voyage simulations of the current situation for comparable vessels. The propulsion system model is then converted, using crude but effective assumptions, to simulate ammonia-diesel operation of the same vessel, mimicking a situation in which the ship, or its main engine, is retrofitted to operate on ammonia-diesel. In this model, the ship has the same direct-drive propulsion system as before, with the same main engine and power output.

After presenting the results for the current situation and a potential near-future situation of ammonia-diesel operation for the DTC container vessel, a new propulsion system model is presented, based on the so-called AmmoniaDrive power plant concept. In this concept, ammonia is used as a fuel for a solid oxide fuel cell, producing hydrogen-rich anode off gas and electric power for the ship's systems and a part of the required propulsion power. The hydrogen in the AOG is used as a combustion promoter in a main propulsion engine that provides the majority of the required propulsion power using ammonia as primary fuel, hydrogen from the AOG as a secondary fuel and a very small amount of HVO diesel pilot fuel as ignition source using Diesel's Compression Ignition concept. The results of this first, early version of a AmmoniaDrive Propulsion, Power and Energy (PPE) system model are presented, after which the integration of such a system in the ship design is investigated by implementing the ammonia storage system as well as the main AmmoniaDrive power plant system components in the ship envelope of the DTC post-Panamax container ship. The impact on the amount of containers that can be carried by the vessel is modest, with only ~3.5% less cargo carrying capacity than the current diesel-fueled container vessel. Due to the crude assumptions made and the differences in the two models, it is not yet possible to quantify the decrease in ammonia consumption of the ship with AmmoniaDrive power plant compared with the ammonia-diesel fueled ship. Harmful emissions are potentially reduced by more than 95%. This is not only the result of switching to ammonia as primary fuel, but also because of a homogenous charge compression ignition, with flame propagation as main combustion principle, in the future ammonia-hydrogen marine IC engine.

1 INTRODUCTION

Different sources, see amongst others [1], [2] and [3], consider combining Solid Oxide Fuel Cells (SOFC) and reciprocating Internal Combustion Engines (ICE) in a Power, Propulsion and Energy system for (large) ships highly advantageous. Limitations and concerns with regards to technical, economical and/or regulatory feasibility have however hindered widescale adoption of this FC-ICE combined power plant concept, especially when fuelled by current marine fuels such as VLS(/H)FO, MD(/G)O or NG.

At the same time, the maritime industry is preparing for the future hydrogen economy by researching and developing ships, and ship technology, that are fuelled by sustainable shipping fuels such as hydrogen, methanol or ammonia. Marine ICEs utilizing DF technology with diesel pilot injection seems to be preferred in industry in the short-term, irrespective of the main (e-)fuel. Conventional DF technology provides good control over combustion progress and satisfactory low load operation. Furthermore, CDF technology that can switch to full diesel mode also enables cost-effective compliance with Safe Return to Port requirements. However, with this option, ships continue to rely, at least partly, on fossil, carbon-based fuels.

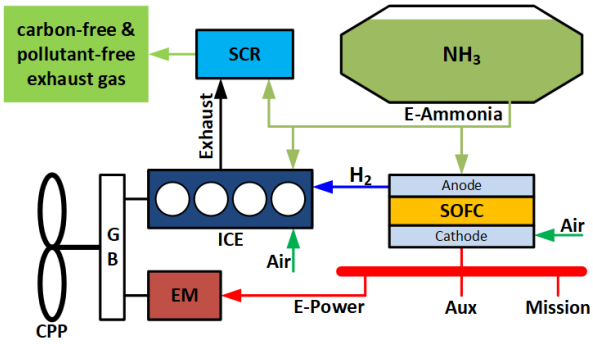

Figure 1. AmmoniaDrive power plant concept, see amongst others [4] and [5].

In contrast, the AmmoniaDrive power plant concept aims to utilize the hydrogen available in the Anode Off Gas (AOG) of a SOFC as combustion promoter in a (mostly) ammonia-fuelled marine ICE. The intention with this concept is to have a completely decarbonised, single-fuel system. Only e-ammonia needs to be bunkered and supplied to the AmmoniaDrive Power, Propulsion and Energy system to supply a ship with mechanical power for propulsion and electric power for auxiliary and mission equipment. The PPE system is expected to have zero harmful emissions, as any unburned ammonia, NO_x, or N_2O formed during combustion is reformed in the SCR to N_2 and H_2O in the exhaust gases.

Combining SOFC and ICE technology in this way and utilising the hydrogen-rich AOG results amongst others in better overall system efficiency, leading to decreased operational costs, which is particularly important given the costs projections of sustainably-produced ammonia. The Ammonia-Drive SOFC-ICE combined system is characterised by trade-off possibilities and optimisation opportunities for different operational profiles as well as different ship design objectives like efficiency, power plant size, transient loading capabilities, investment costs (CAPEX) and operational costs (OPEX). By varying the power split between the SOFC and ICE in the design phase, an optimum can be found for specific operational profiles. Once the power split has been established and the system realised, varying the operational power split between the two power sources provides further multi-objective optimisation possibilities for e.g. system efficiency versus transient capabilities.

For large cargo vessels, like the 14000 TEU Duisburg Test Case (DTC) containership, it seems favourable, see amongst others [4] and [6], to install relatively more ICE power than SOFC power. This solution fits best with the operational profile of such vessels, in which much more mechanical power is needed for propulsion than electrical power for the ship's grid. Furthermore, this solution mitigates impact on the ship design, as ICEs are more power-dense than SOFCs, and CAPEX, as ICEs are expected to remain less costly than SOFCs, while still providing an increase in overall system efficiency. This paper reports on a study in which the PPE system of the DTC containership is designed according to the AmmoniaDrive power plant concept with a power split $P_{ICE} / P_{SOFC} = 3$.

In section 4 and 5, this paper presents a preliminary study on implementing the AmmoniaDrive power plant in the 14000 TEU DTC post-panamax container vessel, providing results of an early version of a time-domain model that can simulate typical voyages, e.g. from Asia to Europe, as well as results of a ship integration study that visualizes the ship design with the AmmoniaDrive power plant and ammonia storage implemented on board of the vessel. We also quantify the penalty on container carrying capacity of the vessel. Furthermore, the paper introduces some of the AmmoniaDrive PhD research projects and how they contribute to meeting the technological and economical challenges associated with introducing such an integrated SOFC-ICE power and propulsion plant in the maritime industry, including impact on crew safety and local environment. The paper starts however with a further introduction of the AmmoniaDrive power plant concept and the DTC containership in section 2. Section 3 introduces a propulsion system model for engine-only

configurations, i.e. without SOFC technology, representing more conventional propulsion system configurations that may be realised sooner, to obtain benchmark results against which the results of the AmmoniaDrive simulations can be compared. In section 6 conclusions are drawn and future research activities are introduced.

2 THE AMMONIADRIVE POWER PLANT CONCEPT AND THE DUISBURG TEST CASE POST-PANAMAX CONTAINER VESSEL

2.1 AmmoniaDrive Power Plant

2.1.1 AmmoniaDrive Research Project

The AmmoniaDrive research project aims to demonstrate the feasibility of the AmmoniaDrive power plant concept, which combines SOFC and ICE technology as explained in the previous section. This power plant concept currently is at a low Technology Readiness Level (TRL) of 1-2; the goal of the AmmoniaDrive research project, with 9 PhD researchers and one post-doc, is to raise this level to 3-4 at the end of the project. Besides this increase in the TRL, an increase in the Societal Readiness Level (SRL) of the concept is aimed for as well, by investigating how to ensure the safety of this solution, how to mitigate the environmental impact of potential ammonia spills, under which economic conditions the power plant concept becomes economically viable for different ship types, etc.

This paper introduces early versions and results of time-domain models of the AmmoniaDrive power plant concept. The results of these simple, but effective, models are also compared to engine-only propulsion system concepts utilising diesel-only or ammonia-diesel as fuel(s). The latter concepts are in fact introduced first in order to be able to compare the AmmoniaDrive equipped vessel with solutions that are technically feasible now or on a shorter term than the combined SOFC-ICE PPE system.

2.1.2 Combining SOFC and ICE technology

Figure 1 showed the basic lay-out of the AmmoniaDrive power plant, excluding any intermediate energy storages, like hydrogen storage or batteries, and support systems for cooling, heat integration, etc. SOFC and ICE technology are combined in such a way that the hydrogen-rich Anode Off Gas (AOG) from the SOFC is used as a secondary fuel for the ICE. This concept was investigated earlier in the GasDrive project, ref. [1], [3] and [7], and lead to a number of promising results, amongst which an improved combustion efficiency for a NG-SI marine-sized engine through the addition of a small amount of hydrogen in the NG-air mixture. Given the challenging combustion properties of ammonia it is expected that the benefits of adding hydrogen to an ammonia-fuelled engine are even larger than for a NG-fuelled one. The ability of hydrogen to significantly improve the combustion properties of ammonia is confirmed by a number of sources, see e.g. [8] and [9]. Where others have already utilised this knowledge by freeing hydrogen from ammonia in a cracker in order to use NH_3/H_2 mixtures in ICEs, AmmoniaDrive uniquely uses a HT SOFC to crack the ammonia into hydrogen and nitrogen.

2.1.3 AmmoniaDrive Power Plant

Starting from the ammonia tanks, see Figure 1, ammonia is fed to the SOFC system, possibly with a pre-reforming step in between (not shown). The majority of the hydrogen released from ammonia is then used by the SOFC to generate electric power for the ship's auxiliary and mission loads. Excess electric power may be used to drive the propeller through an electric motor, or may be stored in batteries (not shown). A significant amount of hydrogen is left unused by the SOFC and exits as one of the constituents of the Anode Off-Gas (AOG). What the exact Utilisation Factor (UF) of the SOFC should be is part of the on-going research and may very well depend on the operational mode of the system, but values from 55 – 85% can be expected.

The hydrogen-rich AOG is subsequently used as a secondary fuel in the ICE, which is primarily fuelled by ammonia from the ammonia tanks. The AOG may be dehumidified before entering the engine (not shown), but whether this is a necessary step is again part of the on-going research. Given that both fuels are gaseous at atmospheric, or slightly raised, pressure and temperature, a pre-mixed concept, where both ammonia and AOG are mixed with the charge air is the most likely candidate with regards to fuel injection strategy. However, alternatives can be thought of as well, which would provide their own advantages and disadvantages, for instance with regard to combustion efficiency and pollutant (NO_x, N_2O) formation. In either case, SCR technology will be required to realise the carbon- and pollutant-free exhaust gases of the ICE(s) shown in Figure 1. Depending on the amount of unburned NH_3 and NO_x in the exhaust gases, a small supply of ammonia from the tanks may be needed for the SCR as well.

Note that an intermediate AOG storage between the SOFC and ICE, which is not shown in Figure 1, may be required to temporarily store hydrogen as well. Furthermore, Figure 1 shows the ICE mechanically driving the propeller through a gearbox, which was only done to demonstrate the system is conceptually thought of as a Power,

Propulsion and Energy system for ships. Alternatives, e.g. with a shaft generator (no gearbox needed), or an all-electric plant where the ICE drives an alternator and propeller drive is fully electric, are obviously also possible. The latter might even be necessary when the propeller is Fixed Pitch Propeller instead of the Controllable Pitch Propeller indicated in Figure 1.

2.2 DUISBERG TEST CASE Container Vessel

[10] describes the geometry as well as resistance and propulsion properties of the so-called Duisberg Test Case (DTC) post-panamax container ship. It "is a hull design of a typical 14000 TEU container ship, developed for benchmarking and validation of numerical methods." According to [10], "DTC is a single-screw vessel with a bulbous bow, large bow flare, large stern overhang and a transom." Figure 2 is copied from the original paper and shows the hull sections of the vessel.

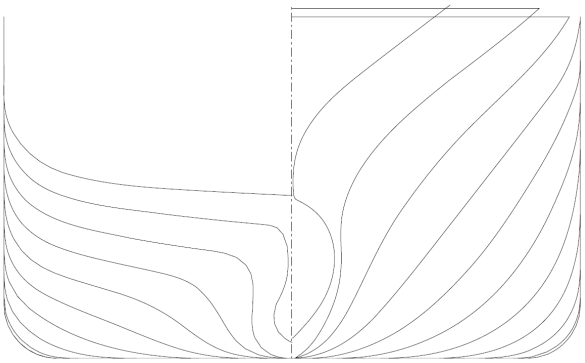

Figure 2. Hull sections of DTC container ship, copied from [10].

In this paper the resistance and propulsion data of [10] are combined with two different engines. One engine for "engine-only" configurations in section three and another engine for the combined SOFC-ICE AmmoniaDrive power plant configuration in section four.

3 ENGINE-ONLY PROPULSION SYSTEM SIMULATION OF DTC POST-PANAMAX CONTAINER VESSEL

For benchmarking it is useful to first have an approximate idea of the fuel consumption and emissions of the current vessel, i.e. a scenario in which the DTC container vessel is realised with a conventional direct-drive propulsion system with a diesel-fuelled (VLSFO) marine 2-stroke engine as main propulsion engine. To do so, the ship resistance and propeller data in [10] is used to determine amongst others the Effective towing Power (P_E) and required Propeller Power (P_p) for different ship speeds and match the propeller to an engine that is currently commercially available.

3.1 Propulsion system model

The propulsion system model used in this section is implemented in Matlab® and Simulink®. The top layer of the model is depicted in Figure 3. From left to right, the first (red), third and fifth blocks represent the main propulsion engine, the propeller and the ship (resistance) respectively. In the blocks in between the acceleration / deceleration of the rotating system (2nd block) and the ship itself (4th block) are calculated and integrated with respect to time in order to derive rotational speed and ship speed respectively at each time step of the simulation. The two main inputs to the model are shown as well: the fuel rack position on the left side and external disturbance factors for added ship resistance on the right side.

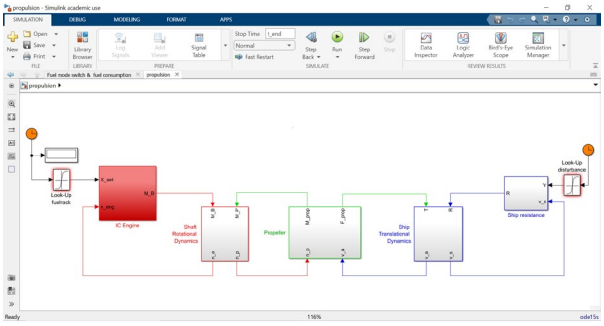

Figure 3. Top layer of propulsion system model.

The propulsion system model is based on a very basic, but fast, effective, and insightful model used in the first year of the Maritime Technology Bachelor of Science program of Delft University of Technology. The model was developed and introduced in [11]. In the first-year course, the model is used and enhanced by students, which enables them to take their first steps in understanding ship propulsion system fundamentals. In the course a different vessel than the one demonstrated here is used as a case study.

3.1.1 Ship Resistance

The ship resistance is calculated as a function of ship speed. The ITTC procedure is used to determine the different non-dimensional resistance components at each ship speed. Equation 1 gives the ITTC 1957 empirical formula for flat plate frictional resistance.

$$C_F = 0.075/(\log_{10} Re - 2.0)^2 \qquad (1)$$

The total non-dimensional ship resistance can then be calculated using Equation 2.

$$C_T = (1 + k) \cdot C_F + C_W \quad (2)$$

In which k is the form factor, the value of which is taken over from [10] as k = 0.145. An extrapolation of the data presented in [10] to lower ship speeds was needed for the non-dimensional resistance component representing wave-making resistance C_W to cover all ship speeds. Figure 4 shows the six data points from [10] above a ship speed of 10 m/s, an added data point of C_W = 0 at a ship speed of 0 m/s to force the fit equation to intersect with the origin and finally the fit equation.

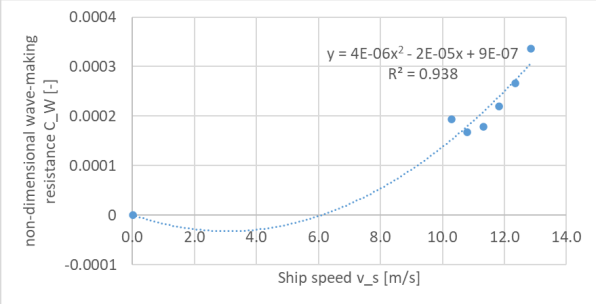

Figure 4. Extrapolation of non-dimensional wave-making resistance component data to lower ship speeds.

It is clear from Figure 4 that the extrapolation is crude and for some ship speeds even impossible, with negative values for C_W at v_s = 0.0 – 6.0 m/s. This will however not have a significant effect on the accuracy of the results, as wave-making resistance is a very small resistance component for these low ship speeds. In fact, for this long vessel, even ship speeds of e.g. 12 m/s still correspond to low Froude numbers, resulting in wave making resistance still being a factor 10 smaller than frictional resistance, see Table 1.

Table 1. Results of resistance model tests, copied from [10].

v_m [m/s]	v_s [m/s]	Fr [-]	Re_m $\cdot 10^{-6}$ [-]	$C_T \cdot 10^3$ [-]	$C_F \cdot 10^3$ [-]	$C_W \cdot 10^4$ [-]
1.335	10.29	0.174	7.319	3.661	3.170	1.932
1.401	10.80	0.183	7.681	3.605	3.142	1.672
1.469	11.32	0.192	8.054	3.588	3.116	1.791
1.535	11.83	0.200	8.415	3.602	3.092	2.194
1.602	12.35	0.209	8.783	3.623	3.069	2.660
1.668	12.86	0.218	9.145	3.670	3.047	3.360

3.1.2 Propeller

The open water propeller data, i.e. dimensionless Thrust K_T and dimensionless Torque K_Q of the propeller, as reported in [10] were fitted using a second degree polynomial. The R^2 value of the fit equations are 0.9998 and 0.9999 respectively, as can be seen from Figure 5.

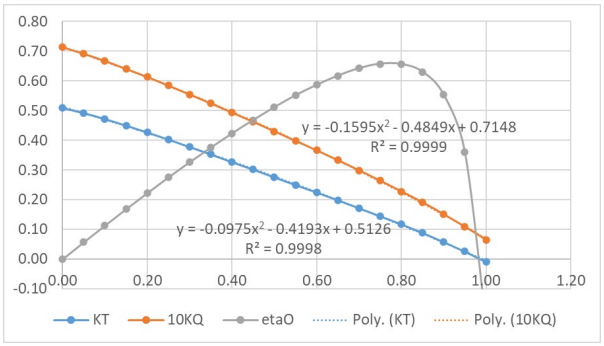

Figure 5. Open water diagram based on data in [10] with 2nd degree polynomial fit equations.

3.1.3 Matching

The relations as introduced above were implemented in a propulsion system model in Simulink®, from which the resulting ship resistance curve and required propeller power for the DTC container vessel at full scale (L_{PP} = 355 m.), as depicted in Figure 6 and Figure 7 respectively, were obtained.

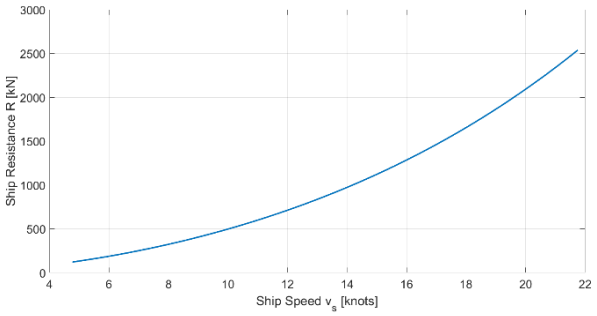

Figure 6. Ship resistance curve.

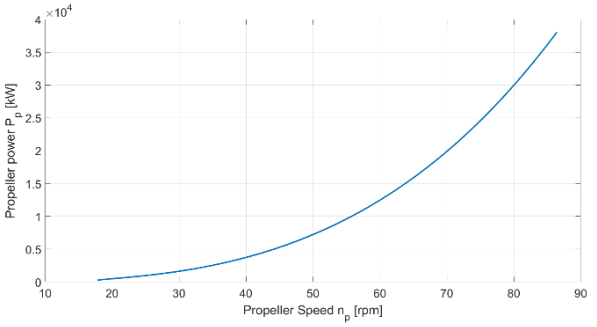

Figure 7. Required propeller power as function of rotational speed.

The propulsion system model is completed with a basic engine model for the main propulsion engine. The data used for the engine model is based on the WINGD X82-2.0 data as retrieved from the website of WINGD [12]. The engine directly drives the full-

scale propeller (D_P = 8.911 m.). The rotational speed of the engine, and therefore the propeller, is limited to 84 rpm. This results in the matching of propeller load line and assumed engine envelope as depicted in Figure 8. Note that the propeller load line has been extended beyond the operational envelope of the engine in this figure, but is limited to operational points in the envelope in the actual propulsion system model.

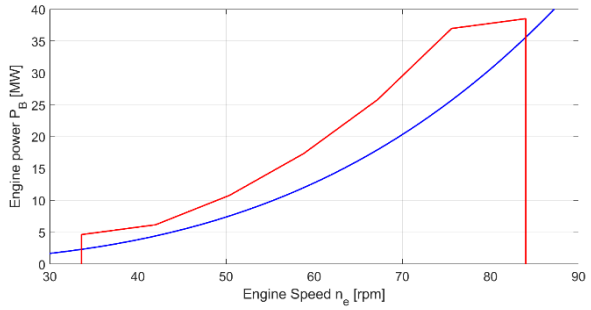

Figure 8. Matching between propeller load line and assumed engine envelope.

This matching leads to a maximum ship speed of approximately 21.2 knots at 84 rpm as maximum rotational speed, and a minimum ship speed of approximately 9.7 knots (both in calm water) at an assumed minimal rotational speed of 33.6 rpm (40% of max rpm) for the engine and propeller.

3.1.4 Engine model

The engine model contains four basic models for combustion losses, heat losses to cooling water and lubrication oil, heat that leaves the engine via the exhaust gases and frictional/mechanical losses. The engine model is depicted in Figure 9.

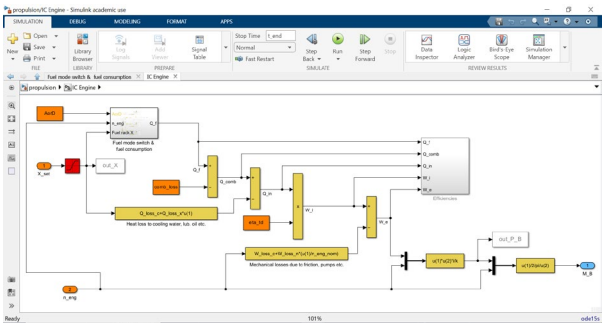

Figure 9. Engine model in Simulink®.

The overall engine efficiency is calculated for each operational point of the engine by using equation 3 from [13].

$$\eta_e = \eta_{comb} \cdot \eta_q \cdot \eta_{td} \cdot \eta_m \quad (3)$$

The specific fuel consumption at Maximum Continuous Rating (MCR) power of this engine (38500 kW) is reported to be 165.3 g/kWh [12]. This value converts to an overall engine efficiency in the nominal MCR point of η_e = 0.51. Together with assumptions for three of the partial efficiencies in equation 3, this information is used to determine the thermodynamic efficiency of the engine in the MCR point.

With regards to combustion efficiency, the model allows for constant combustion losses, but for diesel operation these losses are set to zero, i.e. complete combustion is assumed and η_{comb} = 1.0. The engine model contains two basic functions for heat losses and frictional losses, leading to varying η_q and η_m in equation (3). The heat input efficiency, η_q, is assumed to be 90% in the nominal MCR point of the engine, i.e. 10% of the heat released during combustion is lost to lubrication oil and cooling water via cylinder heads, walls and pistons. This leads to a nominal heat loss which is assumed to consist of a constant part $Q_{loss,c}$ of 40% and a fuel rack dependent part $Q_{loss,x}$ of 60%. These terms are used in a function (see equation 4) that calculates heat losses in each operational point, where X is the fuel rack position, or rather, the percentage of nominal fuel input per cylinder per cycle.

$$Q_{loss} = Q_{loss,c} + Q_{loss,x} \cdot X \quad (4)$$

Likewise, the mechanical efficiency is assumed to be 95% in the nominal MCR point of the engine, leading to a nominal mechanical loss of which 30% is assumed constant and 70% is assumed speed dependent, see equation 5.

$$W_{loss} = W_{loss,c} + W_{loss,n} \cdot \frac{n_{act}}{n_{nom}} \quad (5)$$

Equation 5 shows how the work losses per cylinder per cycle are calculated as a function of engine rotational speed. The work loss is subtracted from the indicated work per cylinder per cycle to arrive at the effective work per cylinder per cycle, which is converted to engine power using the firing frequency, as can be seen from Figure 9.

A constant thermodynamic efficiency η_{td} is assumed for all operating points of the engine, making the heat lost to the environment via the exhaust gases directly proportional to the amount of heat that is effectively available for the closed in-cylinder process. The thermodynamic efficiency is determined to be for the nominal MCR power as 59.65%, based on the above introduced assumptions for losses in the nominal point and the calculated overall engine efficiency of 51% in the MCR point. The overall engine efficiency varies as a function of load as a result of the functions for

heat losses and mechanical losses in equations 4 and 5 respectively, as can be concluded from Figure 10.

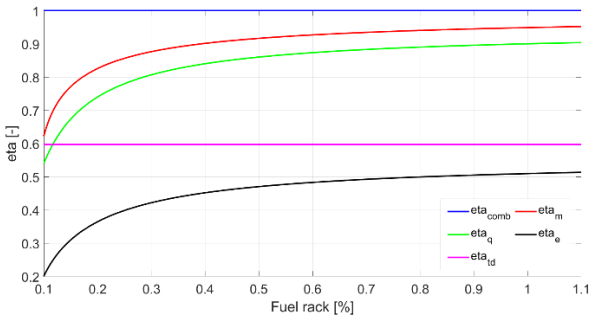

Figure 10. Engine efficiencies in model.

It should be clear to the reader that the basic engine model as introduced here is not correct in the sense that overall engine efficiency is maximal at the highest load point and would in fact continue to increase if the engine model was allowed to operate at loads beyond the nominal point. The model also does not fit well to data for other operational points that may for instance be found in the product guides of engines or FAT tests, as these typically show the highest engine efficiency at loads between 75-85%. Finally, with the assumption of a constant thermodynamic efficiency, the model is even more idealised than ideal cycle models like Otto, Diesel or Seiliger (air-standard dual cycle). Despite such (valid) critiques, the engine efficiency does show a correct trend as well as realistic values for all loads along the propeller load line. Furthermore, it is clear that this basic engine model is not computationally intensive and will be very effective when simulating voyages. This becomes clear in the next section, where the model is used to simulate a voyage of the DTC container vessel from Asia to Europe.

3.2 Diesel-only voyage simulation

The propulsion system model as presented in the previous section can only be used to simulate rectilinear motion of the DTC container vessel. In this section the model is used to simulate a voyage from South-East Asia (e.g. Shanghai) to Europe (e.g. Rotterdam), passing through the Suez Canal.

The objective of the model is not to simulate this voyage in a very accurate manner. It is in fact impossible to quantify the accuracy of the model, as the results cannot be compared to actual measured data (the DTC vessel was, to the knowledge of the authors, never build and data of comparable vessels is not available to the authors). The goal is to have realistic simulation results that enable comparison between different operational modes and power plant configurations. Section 3.1 aimed at introducing the propulsion system model with its underlying physical principles and its crude assumptions to understand the chosen modelling approach and to build confidence in the model by showcasing some important sub-system results. The objective of this section is to further build on this confidence by presenting voyage simulation results that are indeed deemed realistic. Given that all sub-models are based on governing physical principles, the simulation results in fact must be realistic, which the reader may verify in the next section.

3.2.1 Input

The recorded input to the model is depicted in Figure 3. The two main inputs to the model are the fuel rack position X and the disturbance factor Y. The first is quantified as a percentage of the nominal amount of fuel injected per cylinder per cycle. The second is a percentage of added resistance due to e.g. fouling, weather conditions, loading condition of the ship, etc. Note that a lightly loaded vessel, e.g. ballast condition, can lead to a added resistance or disturbance factor lower than 1.0, while e.g. severe weather conditions could lead to a factor higher than 1.0. In the presented simulation the added resistance factor does not change however, not even to simulate shallow water / canal effects in the Suez Canal, and remains constant at 1.0, as can be seen from Figure 11.

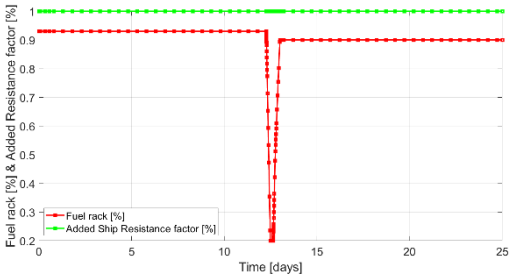

Figure 11. Recorded simulation input variables.

The simulation is kept as simple as possible, to not confuse different simultaneous effects. The only input that really changes is the fuel rack, with a notable dip in the fuel rack around 12 days to simulate the passing of the Suez Canal. The operational limits on the fuel rack set for this simulation are also clear from Figure 11. The upper limit is set to 93% to avoid over-speeding of the engine. This can also be seen from Figure 13 in the next section.

Note that Figure 11 shows a ‘measurement’ of how the input variables X and Y change over time during the simulation. This is clear from the markers that are depicted on the lines. These markers, or rather

the distance between them, give a clear indication of how the variable time step solver that is used in the model adjusts the time step during the simulation. This distance is large, indicating large time steps, when the inputs do not change, while the time step becomes much smaller when an input changes rapidly. The variable time step solver, in combination with the simplicity of the model, makes the model very fast as will become clear in the next section as well.

3.2.2 Main results

Figure 12 shows the main results for ship speed, distance travelled and cumulative fuel consumption for the simulated voyage of 25 days. The total distance travelled is 12519 nautical miles, see the middle graph in Figure 12, which is indeed a realistic value for such voyages; it is in fact a small 20% further than the actual distance between the earlier mentioned ports of Shanghai and Rotterdam.

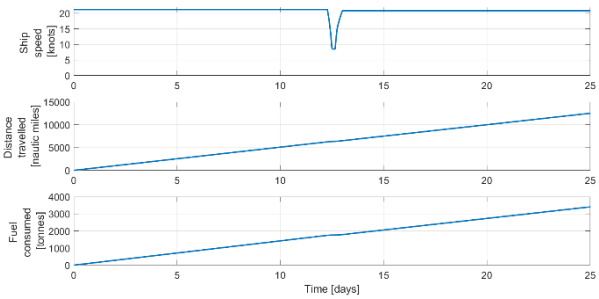

Figure 12. Main output of time-domain simulation of 25 days of sailing on VLSFO diesel fuel.

The bottom graph in Figure 12 shows the cumulative fuel consumption, which ends at 3409 tonnes of diesel consumed. Again this value may be verified by the reader as being representative of actual values for such voyages with comparable vessels, i.e. 14000 TEU post-panamax vessels with a direct-drive propulsion system configuration with a two-stroke, VLSFO-fuelled marine diesel engine.

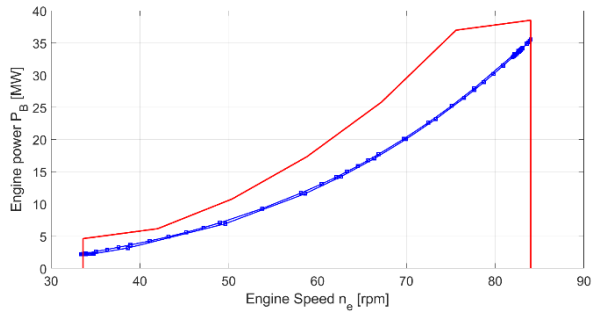

Figure 13. Engine loading during simulation.

Figure 13 shows the load line the engine experiences during the voyage simulation. The engine load is almost the same as shown in Figure 8, but within the limits of the engine and with a small difference between the load line during acceleration compared to the load line during deceleration. This small dynamic effect is caused by the difference in inertia between the rotating propulsion system and the ship itself, where the rotating propulsion system accelerates / decelerates much faster than the ship itself.

Based on the reported results, it may be concluded that the propulsion system model produces representative results, despite the simplicity of the model and the crude assumptions made, especially with regards to the engine model. The models used could be considered the most basic versions of Mean Value First Principle models. The usefulness of such models is not so much in the insights they provide into detailed physical processes, but the speed with which they produce representative results in the time domain. The time it takes to simulate a 25-day voyage of the DTC container vessel is approximately one second on a regular laptop PC with this model, i.e. the model is approximately 2 million times faster than real-time. This indeed provides the user with ample opportunity to change input and settings at will and quickly study the effects of such changes will being able to trust that the results are representative. The model's application opportunities are diverse, from design studies, to control studies, to training of students and crew, etc. Here the focus is to alter the design of the power plant to enable comparison between different PPE system architectures, which we will start with in the next section.

Obviously there is also ample opportunity to increase the level-of-detail of the models to obtain insights and results for questions that require an increase of the model's fidelity. This is part of the AmmoniaDrive research project as well.

3.3 Ammonia-Diesel voyage simulation

3.3.1 Model changes

The previous section showed results for the DTC vessel using only diesel as a fuel. The results may be regarded as representative for comparable vessels that exist nowadays and transport cargo between Asia and Europe. One of the options that may be realised in a relatively short term is to build new vessels or convert existing vessels to operate on Ammonia with a Diesel Pilot injection. Such DF engines, using ammonia rather than NG as primary fuel, are, or will soon become, commercially available. It is therefore interesting to use the propulsion system to simulate ammonia-diesel operation as well.

In this section the input to the model will remain the same, to ensure that results are comparable. This means that the simulated voyage is again 25 days, with the same settings for fuel rack and resistance disturbance factor as reported in section 3.2.1. Since the same vessel is simulated, no changes to the model with regards to resistance and propulsion is needed either. The engine model does need to be adapted to ammonia-diesel DF operation. The engine model as discussed in section 3.1.4. is largely kept the same, but the amount of fuel that is injected per cylinder per cycle needs to be adapted to compensate for two changes: 1) the smaller Lower Heating Value of ammonia and 2) Dual Fuel operation.

The nominal fuel injection per cylinder per cycle in diesel-only mode was determined to be 180.387 grams of VLSFO at MCR power. This value was determined from the reported specific fuel consumption at MCR power and the firing frequency of the chosen WINGD engine. With the LHV of VLSFO (note that in fact the ISO value of 42700 kJ/kg is used in the model and not a more realistic value of e.g. 40500 kJ/kg), it is clear what amount of energy is released from this amount of fuel when combusted. The approach to DF ammonia-diesel operation is to provide the engine per cylinder per cycle with the same amount of energy by choosing an energy share ratio for the two fuels. Based on expectations of the combustion physics of the two fuels involved and reported results by e.g. MAN and other marine engine manufacturers that have built up experience with ammonia-diesel operation of marine ICEs, the energy share ratio chosen at MCR power is 90%-10% ammonia-diesel. To provide 10% of the total energy through diesel pilot injection means injecting 18.0387 grams of diesel per cylinder per cycle at MCR power, i.e. the nominal fuel injection in diesel-only mode divided by ten. The remaining 90% of energy must come from ammonia with an LHV of 18646 kJ/kg, which means a nominal ammonia fuel injection of 371.783 gram.

Having determined the nominal fuel injection of ammonia and diesel fuel for MCR power, the next question is how these values change with engine load. No useful information has been found in public literature to determine realistic values for the energy share ratio between the two fuels at part load of marine ICEs. However, based on the combustion properties of the two fuels and experience with NG-diesel DF engines, it is expected that the energy share ratio of ammonia will quickly decrease with decreasing engine load, i.e. the lower the load of the engine, the lower the portion of total energy input via ammonia and the higher the energy share of diesel. These expectations have been hard-coded in the ammonia-diesel propulsion system model according to Table 2, which shows a linear relationship between the energy share ratio of ammonia and the load of the engine. At a load of 100% the ammonia energy share is estimated at 90% as described before. At 20% load the ammonia energy share ratio has reduced to zero.

Table 2. Energy Share Ratio for ammonia-diesel operation.

Fuel Rack [%]	0.20	0.40	0.60	0.80	1.00
NH3_E [%]	0	0.225	0.45	0.675	0.90

The model contains a look-up table that linearly interpolates between the values of Table 2 and that outputs the end values when the input is higher or lower than the bounds of Table 2, i.e. extrapolation leads to 0% ammonia energy share below Fuel Rack = 0.20 or 90% above Fuel Rack = 100% (obviously extrapolation is not a very relevant scenario). The look-up table is in the sub-system shown in the top left of Figure 9 and is activated by the “switch” AorD. By multiplying the fuel rack position, expressed in a percentage of nominal fuel injection, with the ammonia energy share ratio coming from the look-up table and the nominal fuel injection per fuel, the amount of ammonia and diesel injected per cylinder per cycle is known for each engine load, which enables the same simulation as before.

3.3.2 Main results

As mentioned above the model has the same input and thus simulates the same journey as described in section 3.2.2. This can be concluded from comparing the top two graphs in Figure 14 to the top two graphs of Figure 12. The bottom graph changed considerably though. There are now two lines, one for the diesel pilot fuel, the black line close to the x-axis, and one for cumulative fuel consumption of ammonia, the blue line.

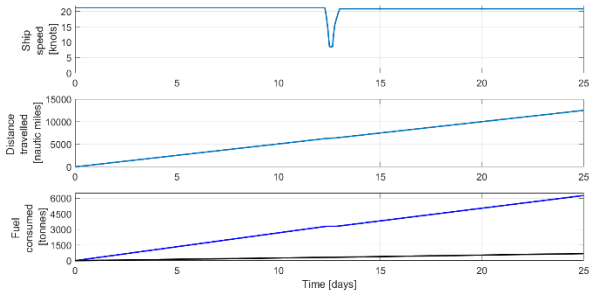

Figure 14. Main output of time-domain simulation of 25 days of sailing on Ammonia-Diesel.

Despite the fact that the propulsion power delivered by the propulsion system is the same as before, leading to exactly the same voyage, the total fuel consumption is obviously a lot higher, owing to the much lower Heating Value of ammonia. The total ammonia consumption is 6257 tonnes and the total diesel consumption is 677 tonnes.

The reduction in diesel fuel consumption is significant, with 80% less diesel consumed than in diesel-only mode, but at the same time perhaps less large than anticipated based on the 90% energy share of ammonia at MCR power. Note however that the engine never runs at MCR power, given the matching shown in Figure 8 and the engine load line as depicted in Figure 13. Since the engine is never at full load the ammonia energy share is always less than 90%. Furthermore, crossing the Suez Canal leads to the engine running at part and low load, where the diesel energy share becomes much larger than the ammonia share. In fact, the small portion of the voyage that the ship sails at a constant low speed, which simulates the actual crossing of the Suez Canal, corresponds to an engine loading of 20% at which the ammonia energy share is exactly zero.

Where the diesel consumption has decreased with 80%, the critical reader may wonder whether the same is true for the GHG emissions of the vessel. This will most probably not be the case as ammonia combustion will likely result in more emission of N_2O, which has a very high GWP compared to CO_2. Furthermore, the current model still assumes complete combustion, of both fuels, and the same engine efficiency. This constitutes an enormous simplification of ammonia-diesel operation that will almost certainly proof to be incorrect.

The current model is too simplistic to provide realistic values of harmful emissions, especially because the amount of harmful emissions formed during the combustion process depends very much on the injection and ignition strategy that will be adopted. Different options for ammonia injection are still being considered and tested, e.g. PFI or LPDI versus HPDI, and it is still unclear which will result in the lowest GHG emissions. Understanding which option should be preferred given different criteria and scenarios (e.g. different engine or ship types) is one of the more detailed goals of the AmmoniaDrive research project.

4 AMMONIA-FUELLED SOFC-ICE PROPULSION SYSTEM SIMULATION OF DTC POST-PANAMAX CONTAINER VESSEL

Since the AmmoniaDrive system combines SOFC and ICE technology, a new model is needed for the DTC vessel with AmmoniaDrive power plant. One of the main system design variables to be decided is the power split between the SOFC and ICE. As [1] and [6] demonstrated, this power split has different and contradicting impact on e.g. overall system efficiency, size of the power plant, transient capability, required investment, etc. Simply put, the more power the SOFC can deliver, the higher the overall system efficiency is, but this also results in higher investment costs, larger area and volume requirements to fit all equipment in the ship and poorer transient response of the power plant. Note that the actual impact of the power split on system properties and key performance indicators are much more complex and contain many uncertainties still, but the basic statement given above is here accepted as a general trend to give direction to the power split choice.

The operational profile of a cargo ship like the DTC container vessel is considered to consist mostly of mechanical propulsion power demand, with a much smaller demand for electric power, especially while sailing at typical container vessel speeds. This leads to a preference of installing relatively more ICE power than SOFC power for these vessels, which is further exacerbated by typical design requirements of having as small as possible machinery rooms, low investment costs and to have an adequate transient response from the propulsion engine. However, especially in the case of ammonia as a fuel, there is also a limit to the power split. Sufficient SOFC power needs to be installed to have sufficient hydrogen in the AOG to ensure proper combustion of the ammonia-hydrogen mixture in the cylinders of the engine.

These considerations lead to a chosen 25%-75% power split, with 25% of installed power coming from a SOFC system as electric power, of which a large amount is assumed to be available for driving the propeller through a shaft generator in PTI mode, and 75% of installed power coming from a MAN 7G80ME-C10.5 as mechanical propulsion power. Note that the benchmark engine has changed because the matching of a hybrid propulsion system is completely different from the engine-only propulsion system configurations described in section 3. Furthermore, the propulsion system and power plant model for the DTC vessel with AmmoniaDrive power plant was implemented in Python rather than Matlab & Simulink. This change of software is mostly for educational reasons, but has also resulted in different modelling approaches, which means the reader should be careful to compare results from this section directly to results in the previous section.

The resistance and propulsion part of the model was for instance changed in such a way that the

ship's resistance is determined with a square curves for trial and service conditions respectively. This leads to the propeller power versus ship speed diagram as depicted in Figure 15. Note that the red dot that indicates the maximum power is the combined power of the chosen internal combustion engine and electric motor that together drive the propeller. With the chosen power split between the SOFC and ICE the total installed power with Fuel Cells becomes 12.15 MW and the total installed ICE power (for propulsion only) becomes 32.69 MW (which indeed is very close to the output power of a MAN 7G80ME-C10.5).

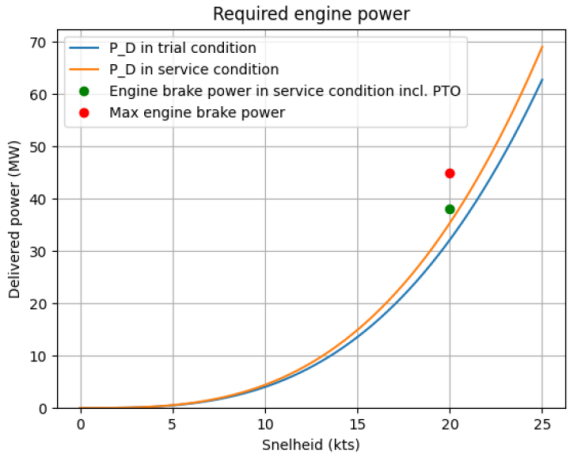

Figure 15. Propulsion power demand and engine rating in AmmoniaDrive propulsion system model.

With regards to the SOFC a choice needs to be made with regards to the installed power. Since Fuel Cells have a much better efficiency at part load it is interesting, from an operational expenditure point of view, to install more power than in needed. However, this of course means that the investment costs become a lot higher, while SOFCs are already very expensive on kW output basis compared to PEMFCs and ICEs. It is therefore chosen to design the SOFC system such that they operate at maximum power on a cell basis when the system delivers the required 12.15 MW. Unfortunately this choice means that SOFC efficiency will not be much higher than the efficiency of a large marine ICE, depending also on the Fuel Utilization factor.

The basis for the Fuel Cell system design is provided by [14], which described the design process of a scalable high-power SOFC unit for maritime applications. The paper first introduces an SOFC unit containing six 22.5 kW stacks. The net rated power of the unit is 125 kW, which is six times 22.5 kW minus the parasitic power needed for the blowers. Nine of such SOFC units are then placed in a SOFC room that supplies 1125 kW of electric power. The SOFC room is 5 meters wide, 2.3 meters high, and 17.1 meters long (including the cold BOP room). The SOFC room is reported to have a power density of 5.7 kW/m^3 or 13.1 kW/m^2. Figure 16 shows a render of such a SOFC room, copied from [14]. The DTC vessel with AmmoniaDrive power plant will be fitted with 11 of such SOFC rooms.

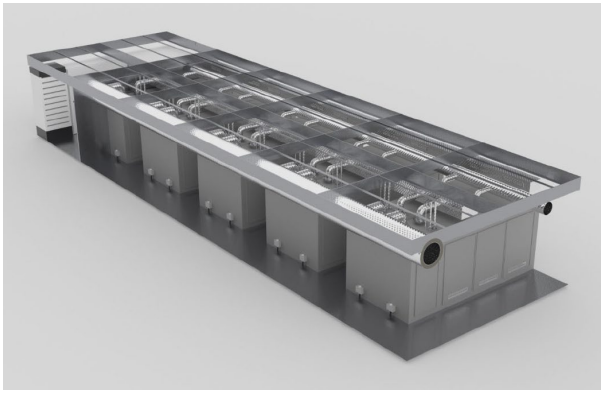

Figure 16. Render of concept design SOFC room for the SOFC unit with COGR, copied from [14].

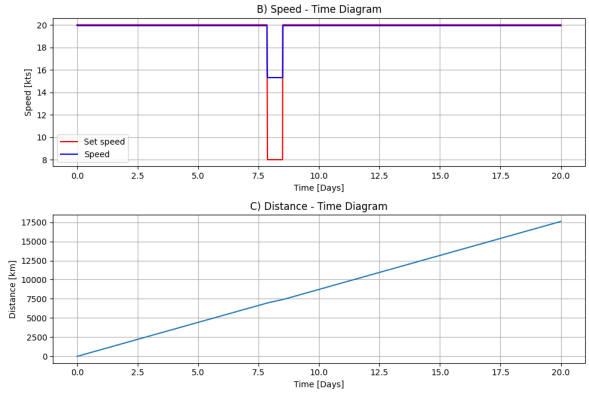

Figure 17. Main output of Python model for AmmoniaDrive power plant on board of DTC vessel.

Figure 17 shows a comparable simulation result as in section 3, but now the idea is that only ammonia is used as a fuel for the ship, see section 2.1. The model used contains however a number of very crude assumptions that still need to be revisited. For instance, the minimum ship speed is over 15 knots, which would be quite an issue in the Suez Canal where there is a speed limit of 8 knots. This low speed was in fact also not reached by the engine-only simulation, but it came much closer and shallow water and canal effects on resistance were completely ignored in those simulations. These effects are ignored in this simulation as well, but this cannot explain the high minimum speed of 15 knots. The current model does not allow for the SOFC units to run at part load, which means a base load of 12.15 MW is always provided to the ship. As

auxiliary power demand and electric losses are not yet modelled adequately either, this power is in fact delivered to the propeller, which does explain the lower speed limit of 15 knots seen in Figure 17.

Together with the relatively low efficiency of the SOFC's and other assumptions that require careful reconsideration, this has resulted in a total fuel consumption that is not representative of what the AmmoniaDrive power plant should be able to achieve. The total ammonia consumption is 6765 tonnes for a voyage of 20 days, with a speed that is typically 20 knots and a total distance travelled of approximately 9500 nautical miles.

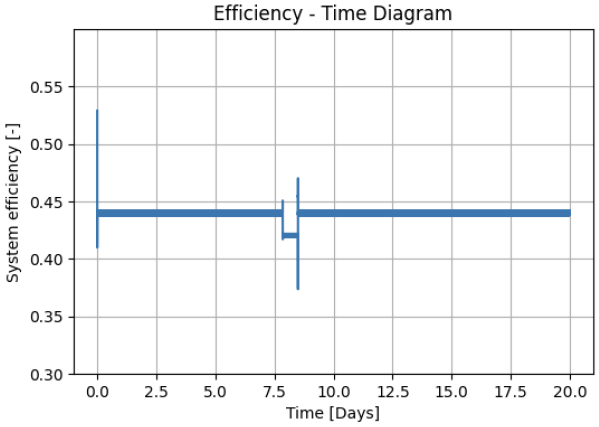

Figure 18. System efficiency as function of time.

This somewhat disappointing result is further substantiated by Figure 18, which depicts on average a total system efficiency lower than 45%, while stationary calculations made for another AmmoniaDrive power plant configuration showed a total system efficiency in excess of 50%, depending on the chosen power split and individual efficiencies of SOFC and ICE. It is clear that the propulsion model needs further development, not only with regard to the level of detail of the component models, but also with regards to some of the assumptions made in the current modelling approach as well as for the power management system. Note for instance that the choice for constant (high) SOFC power output also leads to an ICE that is operating in part load when the set ship speed is not sufficiently high.

Nonetheless, a preliminary version of an AmmoniaDrive propulsion system model was set up in this study. Even though it did not yet adequately show the full potential of the AmmoniaDrive system, it did demonstrate that such a model can produce results that are not completely unrealistic. Furthermore, the study also evaluated the impact of the AmmoniaDrive power plant on the ship's lay-out, which is the topic of the next section.

5 INTEGRATION OF AMMONIADRIVE POWER PLANT CONCEPT IN THE SHIP'S DESIGN

To determine the impact of integrating the AmmoniaDrive power plant in the DTC vessel, a lay-out or general arrangement of the vessel needs to be developed first as [10] only defined the under water part of the vessel. The developed lay-out is based on the general arrangement of 'Al Murabba' found in [15]. Figure 19 shows the potential lay-out of cargo spaces for the DTC vessel when equipped with a conventional diesel-fuelled engine-only propulsion configuration. With this lay-out 15000 TEU can be fitted on board of the vessel.

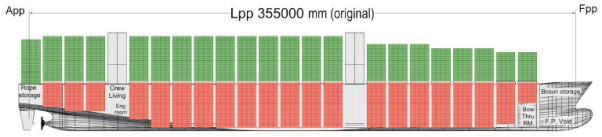

Figure 19. Potential lay-out of cargo spaces to determine container carrying capacity: 15000 TEU.

When integrating the ammonia tanks the current (tentative) regulations for ammonia fuel storage on board with regards to spacing were taken into account. Furthermore, the simulation results of the propulsion system model resulted in sufficient understanding of the amount of ammonia needed (note that multiple simulations took place with different speed settings and voyage duration). The maximum amount of ammonia was then determined to be 12000 m^3 divided over four tanks. Figure 20 shows how these ammonia tanks were integrated in the cargo holds just ahead of the engine room. It is assumed that these spaces can be appropriately ventilated and secured to enable safe storage and handling of ammonia as a fuel. Note that the tank design and integration is crude, missing e.g. tank connection spaces. One or more design iterations are needed before the design would comply with safety regulations.

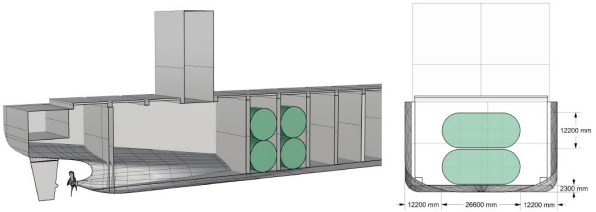

Figure 20. Integration of four 3000 m^3 ammonia tanks at the expense of 514 TEU container carrying capacity.

The cargo holds that were sacrificed for ammonia storage contained 514 TEU in the lay-out shown in Figure 19. This study therefore estimates that the

'penalty' of using ammonia as a fuel on cargo carrying capacity for container vessels is less than 4%.

As a final step, the AmmoniaDrive system components need to be fitted in the ship as well. Integration of these components in the existing engine room seems to be possible, see Figure 21, although it must be noted that this study did not consider the necessary rooms and space for piping of necessary liquids (e.g. fuel treatment, cooling water) and gases (e.g. air), machinery room ventilation, space required for maintenance, etc. A more detailed study of the engine room lay-out may proof to have an impact on the cargo carrying capacity as well, but this impact is estimated to be relatively small compared to the impact ammonia fuel storage has.

This estimation is further substantiated by the reported power density numbers for SOFC and ICE technology. [14] for instance did consider required spacing for auxiliary systems (Balance of Plant components) and maintenance activities, meaning that the SOFC rooms in Figure 21, may proof to be a rather accurate estimation of the space required for SOFCs in the AmmoniaDrive power plant. Furthermore, engine manufacturers report no severe penalty on power density for ammonia-diesel ICE technology, which means the ammonia-hydrogen engine in Figure 21 probably also is a rather accurate estimation of the space required for the AmmoniaDrive ICE.

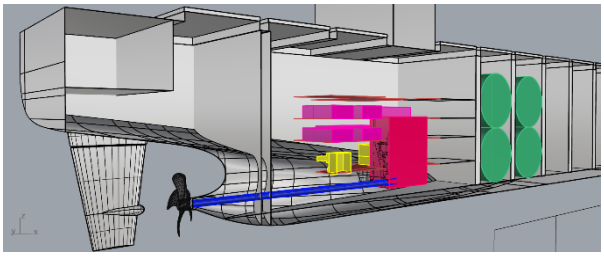

Figure 21. Integration of AmmoniaDrive system components. Ammonia-fuelled SOFC rooms in pink, ammonia-hydrogen-fuelled ICE in red, shaft generator/motor not shown.

6 CONCLUSIONS AND FURTHER RESEARCH

This paper introduced two propulsion system models for ammonia-fuelled post-panamax container vessels using a benchmark vessel for which resistance and propulsion data has been made publicly available. The first propulsion system model is able to effectively simulate long voyages of such vessels when equipped with a conventional propulsion system architecture of a 2-stroke Internal Combustion Engine driving a large propeller directly, i.e. mechanically through a long shaft that connects the engine flange to the propeller. This propulsion system model was used for simulating diesel-only and ammonia-diesel DF operation. Results of the simulations showed realistic values for variables like speed, sailing distance, fuel consumption etc., despite the fact that sub-models must be considered as basic and preliminary versions of Mean Value First Principle models. This provides a solid basis for further development of the models involved.

The second propulsion system model enabled the simulation of the same benchmark vessel, but now equipped with the AmmoniaDrive power plant that combines SOFC and ICE technology to provide ships with both electric power and propulsion power. The simulations again resulted in representative values, but based on earlier stationary calculations better results were expected. Further research must determine whether the earlier stationary calculations were incorrect or whether some of the crude assumptions made in the propulsion system model are the cause of somewhat disappointing results, at least in terms of fuel consumption.

Finally, section 5 demonstrated the results of integrating the innovative AmmoniaDrive power plant into the vessel, from which it was concluded that container vessels switching to ammonia as a fuel must take a cargo carrying penalty of 3-4% into account, mostly for storing sufficient ammonia fuel on board of the vessel.

It should be noted that the AmmoniaDrive power plant concept is still at a low TRL level and fundamental research into its feasibility, from a technical, economical, environmental and safety perspective, is still being performed.

7 ACKNOWLEDGMENTS

This publication is part of the project AmmoniaDrive with project number 14267 of the research programme NWO Perspectief which is financed by the Dutch Research Council (NWO).

8 REFERENCES AND BIBLIOGRAPHY

[1] Sapra, H., Stam, J., Reurings, J., van Biert, L., van Sluijs, W., de Vos, P., Visser, K., Vellayani, A. P., & Hopman, H. 2021. Integration of solid oxide fuel cell and internal combustion engine for maritime applications. *Applied Energy*, 281, Article 115854.
https://doi.org/10.1016/j.apenergy.2020.115854

[2] Elkafas, A. 2024. Hybrid Integration between Solid Oxide Fuel Cell and internal Combustion Engine fueled by clean fuels for domestic vessels

(HISOFCE). Proceedings of *Transport Research Arena*, Dublin, Ireland.

[3] van Biert, L., Visser, K., Negenborn, R., Boersma, B.J., Lammertink, R.G.H., Murk, A.J., & Foekema, E. 2015. Rise to the emission challenge. Gasdrive: Exploring the system integration potential of a LNG fuel cell/gas engine combination, an underwater exhaust and hull resistance reduction. *SWZ Maritime*, 136(10), 19-21.

[4] de Vos, P., Somers, L. M. T., Tinga, T., Foekema, E. M., van der Zwaan, B., Negenborn, R. R. 2022. The AmmoniaDrive Research Project. SWZ Maritime, 143(7/8), 24-27.

[5] Jacobs, I., de Vos, P., Seykens, X.L.J., Negenborn, R.R. 2024. A short review of ammonia Compression Ignition engines for an SOFC-ICE power plant for shipping. Proceedings of *Transport Research Arena*, Dublin, Ireland.

[6] Sapra, H., Stam, J., van Biert, L., de Vos, P., Visser, K., Meijn, G. 2020. Potential of COmbined drive of Fuel cell And Internal Combustion Engine (COFAICE) for naval ships. Proceedings of *International Naval Engineering Conference (INEC)*, IMarEST.

[7] van Biert, L., Woudstra, T., Godjevac, M., Visser, K., & Aravind, P.V. 2018. A thermodynamic comparison of solid oxide fuel cell-combined cycles. *Journal of Power Sources*, Volume 397, Pages 382-396, https://doi.org/10.1016/j.jpowsour.2018.07.035.

[8] Dai, L., Gersen, S., Glarborg, P., Levinsky, H. & Mokhov, A. 2020. Experimental and numerical analysis of the autoignition behavior of NH3 and NH3/H2 mixtures at high pressure. Combustion and Flame, Volume 215, Pages 134-144, https://doi.org/10.1016/j.combustflame.2020.01.023.

[9] Lhuillier, C., Brequigny, P., Contino, F. & Mounaïm-Rousselle, C. 2020. Experimental study on ammonia/hydrogen/air combustion in spark ignition engine conditions. Fuel, Volume 269, 117448, https://doi.org/10.1016/j.fuel.2020.117448.

[10] Moctar, O. el, Shigunov, V., and Zorn, T. 2012. Duisburg Test Case: Post-Panamax Container Ship for Benchmarking, *Ship Technology Research*, 59(3): 50–64. https://doi.org/10.1179/str.2012.59.3.004

[11] de Vos, P. 2015. Design of a New Ship Propulsion System Fundamentals course. Proceedings of *12th International Marine Design Conference* (IMDC). (pp. 281-293). JSNAOE. Tokyo, Japan.

[12] X82-2.0 | WinGD website – data retrieved from September 2024 – January 2025. https://wingd.com/products-solutions/engines/x82-20

[13] Klein Woud, J. and Stapersma, D. 2019. *Design of Propulsion and Electric Power Generation Systems*, IMarEST, London, UK. ISBN: 9781856098496.

[14] Veldhuizen, B., Diethelm, S., Sahnen, D., Thomas, A., van Biert, L. & Visser, K. 2023. Upscaling and Design of an SOFC System for Marine Applications. Proceedings of Indo-Pacific International Maritime Conference, Sydney, Australia.

[15] Speares, S. et al. 2016. Significant Ships of 2015. The Royal Institution of Naval Architects, London, UK.

9 CONTACT

P. (Peter) de Vos PhD, Department of Maritime and Transport Technology, Delft University of Technology, The Netherlands.

p.devos@tudelft.nl